Prediction of CT Saturation Period for Differential Relay Adaptation Purposes

Waldemar Rebizant
Wroclaw University of Technology
Wybrzeze Wyspianskiego 27
50-369 Wroclaw, Poland
rebizant@pwr.wroc.pl

Tammam Hayder
University of Stuttgart
Pfaffenwaldring 47
70569 Stuttgart, Germany
thayder@ieh.uni-stuttgart.de

Ludwig Schiel
SIEMENS AG Berlin
Wernerwerkdamm 5
13623 Berlin, Germany
ludwig.schiel@siemens.com

Abstract: A new approach to CT saturation assessment is presented in the paper. Detailed algorithms for decaying DC component measurement and CT saturation prediction are proposed and their accuracy is discussed. The information on CT saturation period is further used for adaptation of the generator / transformer differential protection. Improved stabilization for external faults is achieved by appropriate temporal adjustment of the differential curve for the time period of CT saturation. The protection developed was tested with both EMTP-generated and real world registered current signals.

Index Terms: CT saturation, differential protection, digital signal processing, measurement of decaying DC parameters, synchronous machine, transformer.

I. Introduction

EVEN though the differential relays are considered quite reliable and robust, there are situations when they may malfunction. Contradictory requirements of high sensitivity and selectivity can not reconcile in cases of faults with small through currents which may evoke over-tripping if the CTs saturate due to content of DC component with high value of decaying time constant. Such conditions may arise e.g. during external faults close to generator-transformer units when the time constant T_N is as high as 200-300ms. Sample signals observed during such faults are shown in Fig. 1b. Contrary to high amplitude faults when the CTs saturate within first half-cycle or full-cycle after fault inception (Fig. 1a), the saturation effects for DC-induced cases appear only few cycles later and have somewhat different nature. One can observe (Fig. 1b) that the negative half of the signal wave is also falsely transformed to the CT secondary side.

In Fig. 2 sample waveforms of DC components from CT primary and secondary side as well as resulting magnetizing current and flux density in the CT core are given, corresponding to the case of CT saturation due to DC component from Fig. 1b. One can see that in such a case the total flux density B does not rise suddenly at the beginning of fault but becomes higher and higher gradually as an effect of magnetizing with the growing DC component of the current I_μ. In the case presented the critical value of flux density when the CT becomes saturated is reached after approx. two cycles from the beginning of fault.

An illustration of the differential protection operation (in traditional, non-adaptive as well as adaptive versions) for the situations described is given in section IV. It is shown that due to the reasons mentioned relay maloperation (over-tripping) could occur. Thus application of the adaptivity idea is indispensable to assure proper operation of the protection for external faults with small through currents accompanied with CT saturation due to DC component.

In the following chapters the general idea of adaptive protection together with the detailed information on the algorithms of current parameter estimation, CT operation prediction and determination of the necessary adaptation degree are described. The main attention is paid to the procedures of CT saturation assessment, which bring key information for further protection adaptation.

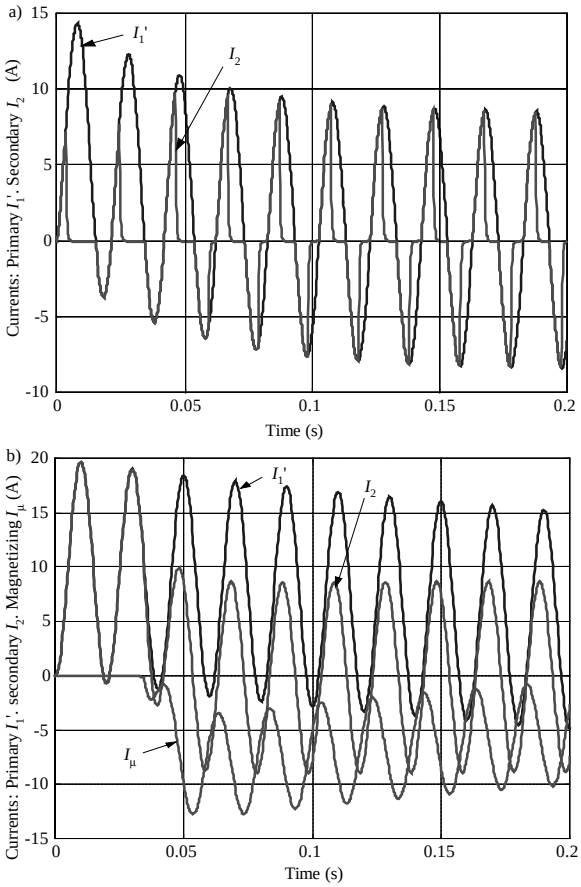

Fig. 1. Primary, secondary and magnetizing currents of a CT during: a) high amplitude faults, b) generator-close fault with small through current.

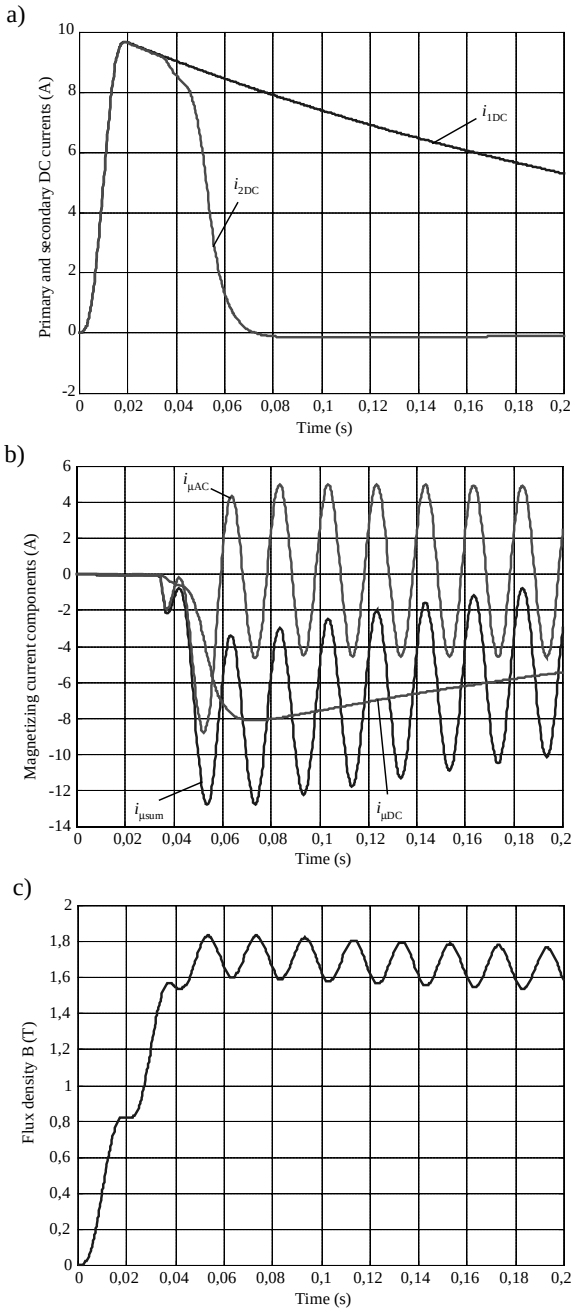

Fig. 2. Currents and flux density components of a CT under fault conditions: a) DC components of primary and secondary currents, b) components of the CT magnetizing current, c) components of flux density in the CT core; $I_1=2I_{n1}$, $I_{DC}=I_1$, T_N=300ms.

II. CT Saturation Assessment

The evaluation of CT saturation period is necessary if the adaptivity concept is to be implemented in practice to get required improvement of the differential protection operation. It is to be emphasized that a kind of CT saturation prediction procedure has to be developed since the traditional saturation detection methods (e.g. as described in [1, 2]) are not able to recognize the situation until it appears. Furthermore, before suitable formulae for calculation of time to saturation and its end can be fired, the fundamental frequency component amplitude as well as the level of decaying DC is to be evaluated. The following subsections unfold the problems of choosing appropriate algorithms for the purpose.

A. Measurement of DC component parameters

The research conducted has included examination of various algorithms for calculation of DC component parameters, i.e. its amplitude I_{DC} and time constant T_N. Both parameters are further used as input data for the adaptive protection procedure described. In the literature the following methods for DC component filtering (rejection) and/or measurement can be found:

- Filtering (rejection) of decaying DC component (with only coarse or without measurement of its parameters) is often performed with application of band-pass or high-pass filters of FIR type [3] (non-recursive filters having sine and cosine data windows or just a cosine filter) or the so called mimic filters [4].
- Least error squares based methods [5] in recursive or non-recursive versions are also used to filter out the DC component that is either taken or not taken into consideration as a part of the signal model.
- State space algorithms, where the DC component is considered as one of the state variables, have a special mixed rejection-measurement character; examples of the algorithms of this kind are the state observer and the Kalman filter [6, 7], with a common weakness related to the necessity of knowing the statistical features of the signal to be measured and its expected noises.
- Algorithms for elimination and partial measurement of the DC component based on the assumption of a detailed deterministic signal model and modified half- or full-cycle filters (Fourier or Walsh functions) [8, 9, 10].

Below three algorithms belonging to the last group of estimators are described and their accuracy and dynamics are analyzed.

The algorithm described in [8] is based on signal filtering with half-cycle Fourier filters (HCDFT). The equations for determination of decaying DC component parameters are as follows:

$$T_N = qT_p = -\frac{T_p}{\ln(Q)} \tag{1}$$

and

$$I_{DC} = \frac{N\left[i_c(N/2) - i_c(N/2+1)\right]}{4\cos(2\pi/N)Q(1+Q^{N/2})}, \tag{2}$$

where

$$Q = e^{-1/q} = \frac{\left[i_c(N/2+2) - i_c(N/2+2)\right]\cos(2\pi/N)}{\left[i_c(N/2+1) - i_c(N/2)\right]\cos(4\pi/N)}, \tag{3}$$

i_c – current signal after filtering, T_p – sampling rate and N – number of samples in one cycle of fundamental frequency.

The algorithm described in [9] is based on full-cycle filtering with first order Walsh function (W1), which in recursive form is given by the formula

$$i_{w1}(k)=i_{w1}(k-1)+wal_1(k)\left[i(k)+i(k-N/2)\right]. \quad (4)$$

The sought time constant T_N is then calculated from

$$T_N = -\frac{T_p}{\ln[r(k)]}, \quad (5)$$

with the coefficient *r(k)* defined as

$$r(k)=\frac{\left|i_{w1}(k)-i_{w1}(k-1)\right|}{\left|i_{w1}(k-1)-i_{w1}(k-2)\right|}. \quad (6)$$

With this method correct estimation results of T_N are expected after $k=N/2+1$ sampling periods counted from the fault inception moment, at the earliest. The coefficient *r* is often additionally limited upwards to the level of 1.0 and, downwards, with a lowest reasonable time constant T_N=4ms. The initial value of DC component is here determined from

$$I_{DC}=\frac{r(k)}{2}e^{kT_p} \quad (7)$$

with the exponential term in (7) introduced to compensate for the time going by.

The algorithm based on full-cycle signal averaging (which corresponds to filtering with the 0-th order Walsh filter – W0) can be expressed in recursive form as [10]

$$i_{w0}(k)=i_{w0}(k-1)+wal_0(k)\left[i(k)+i(k-N)\right]. \quad (8)$$

Coefficient *r(k)* dependent on the decaying DC time constant is further calculated as

$$r(k)=\frac{i_{w0}(k)}{i_{w0}(k-1)}. \quad (9)$$

The value of time constant T_N is then obtained as previously, i.e. from eq. (5), while the initial value of DC component is calculated from

$$I_{DC}=\frac{i_{w0}(k)}{\sum_{n=0}^{N-1} r(k-n)^n}e^{kT_p}. \quad (10)$$

Accurate measurement results are here guaranteed when $k=N+1$ current samples after fault inception are available.

The above-described algorithms for DC component parameters calculation have been extensively tested for accuracy with the signals defined arbitrarily in MATLAB as well as with signals from EMTP-ATP simulations and current signals from fault recorders installed in a real network. The results of DC parameters measurement with the algorithms mentioned for three chosen fault cases are gathered in Table I (description of the cases under the Table). It is seen that all the algorithms are almost perfect for the signals that are not contaminated by any additional components. For real cases, however, when some harmonics or other noise is present in current signal their accuracy is lower. Ranking positions assigned according to the level of measurement errors clearly indicate that the best performance is expected when the full-cycle averaging algorithm (W0) is used.

TABLE I. ERRORS OF DC PARAMETERS MEASUREMENT

Case	Measurement errors for I_{DC}	Algorithm used		
		HCDFT (2)	**W1 (N/2) (7)**	**W0 (N) (10)**
1	absolute [A]	0,0	0,05	0,1
	relative [%]	0,0	1,7	0,3
2	absolute [A]	0,9	0,4	0,1
	relative [%]	40,9	18,2	4,5
3	absolute [A]	0,14	0,04	0,02
	relative [%]	8,2	2,3	1,1
	Ranking	**3**	**2**	**1**

1) Current defined in MATLAB: T_N=300ms, I_{DC}=3A, I_1=5A, f=50Hz
2) Fault current (EMTP-Simulation): T_N=20ms, I_{DC}=2,2A, I_1=3,9A, f=50Hz
3) Current at the generator terminals (real fault case): T_N=120ms, I_{DC}=1,7A, I_1=3,8A, f=60Hz

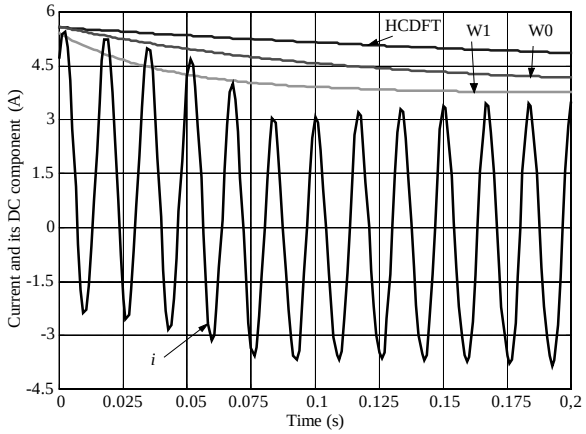

Fig. 3. Comparison of DC parameters estimation with various measurement algorithms for the real fault case (No. 3, description under Table I).

The DC parameters measurement process is illustrated also in Fig. 3 for a chosen real current signal from the generator terminals (case No. 3 – close external fault with CT saturation due to DC component with high time constant). The best estimation results are obtained for the algorithm W0, which is seen especially up to some 35ms after fault inception before the CT saturation begins. It is to be mentioned that the estimation of DC parameters was done only once – just at the beginning of fault, which explains further discrepancy between the signal and its estimated DC component.

The analyses described allowed finding acceptance for the algorithm W0 for further use in the adaptive relay described.

B. CT saturation prediction

The problems related to quality (accuracy) of primary current transformation to the secondary side of conventional CTs during severe saturation of their core have already been described in several papers, e.g. [11], [12], as well as in international standards [13]. The relationships given below originate from the references mentioned, with certain modifications introduced by the authors of this paper to match them to the saturation phenomena due to DC component.

The estimation of CT saturation starting time (t_{S1}) can be done with use of one of the following three relationships:

a) Non-linear formula for the magnetic flux density B_s at the beginning of saturation period [11]

$$B_s=\frac{\mu w_2 I_2}{l}\left(\frac{T_N}{T_W-T_N}(e^{-t_{s1}/T_W}-e^{-t_{s1}/T_N})\right), \tag{11}$$

solvable for the time t_{s1} e.g. with the least error squares method. Herein are: μ – magnetic permeability of the iron core, w_2 – number of turns of the secondary winding, l – middle length of magnetic force lines in the CT iron core, I_2 – amplitude of the secondary current (fundamental frequency component), T_W – CT time constant, T_N – time constant of the network seen from the fault point (equivalent to time constant of DC component in fault current).

b) Simplified version of (11), with CT time constant T_W assumed as infinite (significantly higher as the network time constant T_N), in the form

$$t_{s1}=-T_N\cdot\ln\left(1-\frac{B_S\cdot q}{T_N\cdot R_2\cdot I_2}\right), \tag{12}$$

c) Formula proposed in IEEE Standard C37.110-1996 [13]:

$$t_{s1}=\frac{-(X/R)}{2\pi f}\cdot\ln\left(1-\frac{K_s-1}{(X/R)}\right)=-T_N\cdot\ln\left(1-\frac{K_s-1}{\omega T_N}\right), \tag{13}$$

with $K_s=\frac{V_{sat}}{I_2\cdot(R_2+R_s+Z_b)}$ – saturation factor, X, R – reactance and resistance of the network at the fault spot, R_2 – resistance of the CT secondary winding, R_s – resistan-ce of the leads, Z_b – apparent impedance of the CT burden.

From the magnetic flow law

$$B_s=\frac{\mu}{l}w_2 i_s', \tag{14}$$

by $i_s=I_{DC}e^{-t_{s2}/T_N}$ (neglect of ampere turns due to fundamental frequency current), one can derive a formula for the CT saturation end time (t_{s2}) in the form

$$t_{s2}=T_N\ln\left(\frac{\mu w_2 I_{DC}'}{l\ B_s}\right). \tag{15}$$

The flux density value B_s leading to CT saturation and the maximal expected flux density level B_{max} in the CT core may be determined as [12]

$$B_s=\frac{\mu}{l}\frac{w_1 K_n I_{n1}}{\omega T_W}, \tag{16}$$

$$B_{\max}=\frac{\mu}{l}w_2 I_2\left[\left(\frac{T_N}{T_W}\right)^{\frac{T_W}{T_W-T_N}}+\frac{1}{\omega T_W}\right], \tag{17}$$

whereas the time constant T_W can be calculated from the CT parameters as follows

$$T_W=\frac{L_W}{R_W}=\frac{L_0+L_s+L_b}{R_2+R_s+R_b}. \tag{18}$$

Needless to say, the application of the above-presented formulae is possible in dependence on the availability of the CT and network parameters.

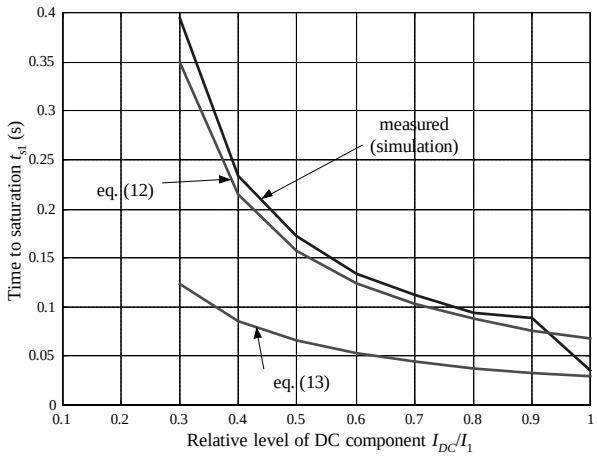

Fig. 4. Time to saturation as a function of I_{DC} and I_1 – comparison of measurement and calculation results for the case $I_1=2I_{n1}$.

To evaluate the quality of the formulae for t_{s1} and t_{s2} calculation a number of simulation tests have been conducted. A variety of simulation cases with diverse combinations of fundamental frequency and decaying DC components amplitudes and time constants were prepared. Introductory analyses and simulative investigations have shown that the values obtainable with formula (12) are very close to those resulting from simulation of CT operation and real-world recordings. The outcomes of equation (13) are usually underestimated, i.e. smaller than in reality (Fig. 4). That means the IEEE standard formula delivers rather conservative values of t_{s1}, being (in our case) situated on the right side in

the sense of eventual adaptation being realized somewhat earlier than really required. On the other hand, the formula (13) is the only one that may be applied in the cases when precise data on required CT parameters is not available.

III. Adaptive Differential Protection

The adaptive approach to the differential protection developed is summarized in Fig. 5. The procedure of adaptive adjusting of the differential characteristic consists of the following steps:

- Calculation of the initial value (amplitude) I_{DC} and time constant T_N of the decaying DC component as well as the amplitude of the current fundamental frequency component I_1 for the time instant just after fault inception,
- Calculation of the expected CT saturation period, i.e. time instants t_{s1} and t_{s2} of saturation beginning and fizzling out,
- Determination of the necessary level of adaptation for given fault case (shifting up of the differential curve or slope changing of the stabilizing section),
- Measurement of the through current amplitude values (differential curve adjusting takes place for fault currents close to nominal ones, i.e. up to $3I_n$),
- Execution of the on-line adaptation of the differential curve for the time period $[t_{s1}, t_{s2}]$.

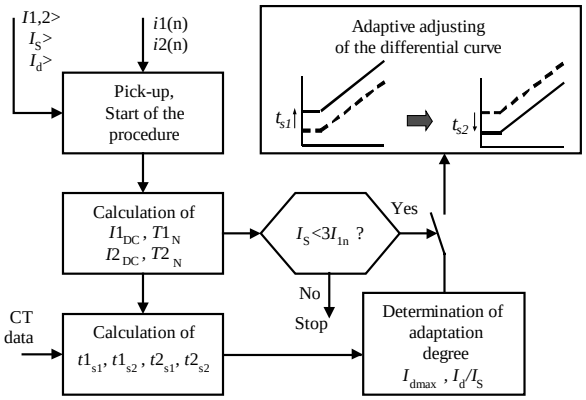

Fig. 5. Block scheme of the adaptive protection.

It is worth to notice that the calculation of mentioned above values is performed for the signals from CTs at both sides of the protected plant (big indexes 1, 2 – Fig. 5). The adaptation is carried into effect at or slightly before the predicted time instant of CT saturation (lower from both calculated values is accepted for this purpose). The detailed equations for the expected values of I_{dmax} and ratio I_d/I_s, in dependence on CT saturation beginning t_{s1} or saturation duration t_{s2}-t_{s1}, may be found in [14].

IV. Relay Testing

The developed adaptive protection has been tested with simulation and real-world recorded fault signals. Below one example of its operation for an external fault is presented. The fault occurred close to generator terminals and was accompanied with DC induced CT saturation.

In Fig. 6 the current signals from both sides of the protected generator (secondary signals, phase L1) are shown with additionally superimposed DC component. One can see that the DC parameters (calculated according to (5) and (10)) are found quite correctly, since the DC curve follows closely the maxima of current waveforms, especially for the time period before CT saturation for which the values were determined. Higher values from those calculated for currents

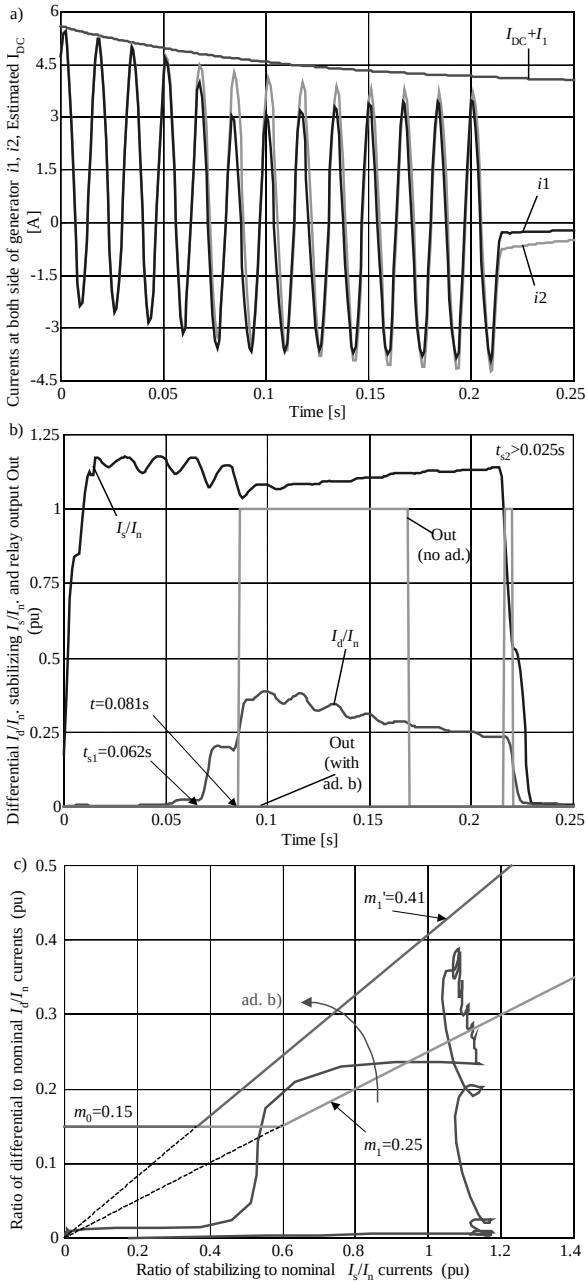

Fig. 6. Operation of the proposed adaptive differential protection for a real-world registered external fault case: a) current signals and estimated DC component, b) differential and stabilizing currents, protection output signals, c) adaptive adjustment of the differential curve in the I_d=f(I_s) plane.

at both generator sides were taken as input variables for calculations at further adaptation steps.

The effects of adaptive adjusting of the differential curve can be seen in Fig. 6b and 6c. Appropriate changes (version b – setting new value of the stabilizing slope) were introduced at time instant $t_{s1\_(12)}$=62.3ms, i.e. before the non-adaptive relay picks up (curve Out (no ad.) in Fig. 6b). The calculated end-of-saturation time $t_{s2\_(15)}$=363ms was greater than the time range presented in Fig. 6. The newly set stabilizing slope fulfilled the expectations, i.e. the stabilization conditions have been significantly improved and unwanted tripping for the external fault was avoided.

V. Conclusions

A new comprehensive approach to differential protection of generator and transformer taking into account CT saturation due to slowly decaying DC component is described. Detailed algorithms for determination of the required parameters of DC component as well as prediction of the coming CT saturation are presented. The adaptive procedure developed includes appropriate on-line modifying of the relay differential curve, thus enabling improvement of protection stabilization for the cases of close external faults accompanied with DC current of high time constant. Testing of the developed adaptive procedure with EMTP simulated and real-world current signals proved much better relay performance when compared to traditional relay version without adaptation.

VI. References

[1] M. Saha, J. Izykowski, M. Lukowicz and E. Rosolowski, "Application of ANN methods for instrument transformer correction in trensmission line protection", in *Proc. of the 7th Conf. on Developments in Power System Protection*, Amsterdam, the Netherlands, April 2001, pp. 303-306.

[2] Y. Kang, S. Kang and P. Crossley, "An algorithm for detecting CT saturation using the secondary current third-difference function", in *Proc. of* the *IEEE Bologna PowerTech Conference*, Bologna, Italy, June 2003, pp. 320-326.

[3] A.G. Phadke and J.S. Thorp, *Computer relaying in power systems*, John Wiley & Sons Inc., 1988.

[4] G. Benmouyal, "Removal of DC-offset in current waveforms using digital mimic filtering", *IEEE Transactions on Power Delivery*, Vol. 10, No. 2, April 1995, pp. 621-628.

[5] M. Sachdev and M. Nagpal, "A recursive least error squares algorithm for power system relaying and measurement application", *IEEE Transactions on Power Delivery*, Vol. 6, No. 3, 1991, pp. 1008-1015.

[6] E. Rosolowski and M. Michalik, "Fast identification of symmetrical components by use of a state observer", *IEE Proceedings – Part C: Generation, Transmission and Distribution*, Vol. 141, No. 6, November 1994, pp. 617-622.

[7] A.A. Girgis and R.G. Brown, "Application of Kalman filter in computer relaying", *IEEE Transactions on Power Apparatus and Systems*, Vol. 100, No. 7, 1981, pp. 3387-3397.

[8] Jyh-Cheng Gu and Sun-Li Yu, "Removal of DC offset in current and voltage signals using a novel Fourier filter algorithm", *IEEE Transactions on Power Delivery*, Vol. 15, No. 1, January 2000, pp. 73-79.

[9] E. Rosołowski, J. Iżykowski and B. Kasztenny, "A new half-cycle adaptive phasor estimator immune to the decaying DC component for digital protective relaying", in *Proc. of the 32nd Annual NAPS-2000*, Waterloo, Canada, October 23-24, 2000, pp. 2-17 - 2-24.

[10] E. Rosołowski and J. Iżykowski, "Adaptive supressing of decaying DC component from relaying input signals", *Techniczna Elektrodinamika, Problemy Sycasnoj Elektrotehniki*, part 7, Kiev 2000, pp. 82-87.

[11] A. Fischer and G. Rosenberger, "Verhalten von linearen und eisengeschlossenen Stromwandler bei verlagerten Kurzschlußströmen", *Elektrizitätswirtschaft*, Jg. 67 (1968), Heft 12, pp. 310-315.

[12] A. Wiszniewski, *Przekładniki w elektroenergetyce*, WNT, Warszawa, wyd. I - 1982, wyd. II – 1992.

[13] ANSI/IEEE C37.110 Standard: IEEE Guide for the application of current transformers used for protective relaying purposes.

[14] W. Rebizant, K. Feser, T. Hayder and L. Schiel, "Differential relay with adaptation during saturation period of current transformers", Paper accepted for the *Power System Protection Conference PSP'04*, Bled, Slovenia, September 2004.

VII. Biographies

Waldemar Rebizant was born in 1966 in Wroclaw, Poland. He received M.Sc. and Ph.D. degrees (both with honors) from Wroclaw University of Technology, Poland in 1991 and 1995, respectively. Since 1991 he has been a faculty member of Electrical Engineering Faculty at the WUT. In June 1996 he was awarded Siemens Promotion Prize for the best dissertation in electrical engineering in Poland in 1995. In 1999 he was granted a prestigious Humboldt research scholarship for the academic year 1999/2000. In the scope of his research interests are: digital signal processing and artificial intelligence for power system protection purposes.

Tammam Hayder was born in Lattakia, Syria, in 1968. He studied Electrical Engineering at the University of Tishreen Lattakia, finishing with the Dipl.-Ing. degree in 1992. At the moment, he is Ph.D. student at University of Stuttgart, Germany, Institute of Power Transmission and High Voltage Technology (email: thayder@ieh.uni-stuttgart.de). His area of research interest is power system protection.

Ludwig Schiel was born in Weimar, Germany, in 1957. He studied Electrical Engineering at the Institute of Technology Zittau, finishing with the Dipl.-Ing. degree in 1984. In 1991 he received the Dr.-Ing. degree. In the same year he joined the Siemens AG, Germany, Department of Power Transmission and Distribution, Power Automation. He is project manager of transformer differential protection systems.